

**The Effects of PMP22 on Gene Expression throughout
Development**

by

Bethany Andrews

Departmental Honors Thesis

The University of Tennessee at Chattanooga

Biology

Project Director: Dr. Margaret Kovach

Examination Date: March 23, 2007

Dr. Ethan Carver

Dr. Henry Spratt

Dr. Manuel Santiago

Examining Committee Signatures:

Project Director

Department Examiner

Department Examiner

Liaison, Departmental Honors Committee

Chairperson, University Departmental Honors Committee

ABSTRACT

Introduction

Charcot-Marie-Tooth disease (CMT) is an autosomal dominant disorder characterized by progressive peripheral neuropathy most commonly caused by a gene duplication of the PMP22 gene mapped to chromosome 17. A clinical and genetic variant of CMT is associated with profound and progressive sensorineural deafness. Molecular analysis identified a unique point mutation in the gene PMP22 instead of the common duplication. Although expression of PMP22 is highest in myelin-forming Schwann cells where it is proposed to function in proper myelination of nerves, its transcript is also detected in non-neural tissues, particularly at critical developmental time-points. PMP22 is a member of the family of growth arrest specific (Gas) genes, which have been shown to regulate gene expression, cell death, and cell division. The purpose of this study is to dissect the molecular pathology of deafness using the Trembler-J mouse as a model of PMP22-associated auditory dysfunction.

Materials and Methods

Differential Display (DD) technology was used to characterize gene expression patterns in normal and Trembler-J mice in order to identify gene transcripts up-regulated or down-regulated relative to quantitative and/or functional levels of PMP22 gene expression. Differential Display was carried out with 2 sets of upstream arbitrary primers (8 primers/set) which are predicted to

represent approximately 50% coverage of all the transcripts present in the sample.

Results

Through DD analysis of wild type and Trembler-J lung tissue, 74 differentially displayed transcripts were identified. Of these transcripts, 63/74 (85%) were down-regulated and 11/74 (15%) were up-regulated. Combinations of anchor primers H-TG and H-TC with arbitrary primers 1, 2, 3, 4, 5, 6, 9, and 12 produced all 74 differentially regulated transcripts. Interestingly, anchor primer H-TA did not generate any differentially displayed transcripts. PCR analysis of DD products resulted in amplification of 60 out of the 74 transcripts. Currently, these PCR products are being cloned for DNA sequence analysis. Once DNA sequence data is retrieved, BLAST homology searches against the mouse genome database will be employed to identify the DD transcripts.

Conclusions

We have identified a set of differentially expressed transcripts associated with defects in the PMP22 gene. DNA sequencing of these transcripts will allow the identification of a set of genes differentially regulated by PMP22. These genes can then be grouped according to structure and function. This comparative analysis of gene expression profiles should aid in the creation of a model for understanding the role of PMP22 during developmental time points. This will further the understanding of PMP22 function and its

interaction with other genes and gene products, and most importantly shed light on its influence of inner ear development and function.

ACKNOWLEDGEMENTS

I would like to thank Dr. Kovach for being my Departmental Honors project director and Dr. Carver, Dr. Spratt, and Dr. Santiago for serving on my committee. I would also like to thank Tonya Carver for her assistance in the lab. Finally, I would like to thank the UHON faculty and my fellow students for their continued support of my academic endeavors.

TABLE OF CONTENTS

I. ABSTRACT.....	2
II. ACKNOWLEDGEMENTS.....	5
III. LIST OF FIGURES.....	8
IV. LIST OF TABLES.....	10
V. INTRODUCTION.....	11
A. Review of Hereditary Neuropathies.....	12
B. Charcot-Marie-Tooth (CMT).....	13
C. Physical Characteristics of CMT.....	14
D. Causes of CMT.....	15
E. Clinical and Genetic Heterogeneity of CMT.....	17
F. Diagnosis of CMT.....	22
G. Treatment of CMT.....	23
H. Genetics of Deafness.....	24
I. CMT and Deafness.....	25
J. Peripheral Myelin Protein (PMP22).....	26
K. Growth Arrest Specific (gas) Genes.....	28
L. Trembler-J Mice as a Model for CMT1A.....	29
M. Purpose of Project.....	33
VI. MATERIALS AND METHODS.....	34
A. Trembler-J Mouse Model and Animal Care and Use.....	35
B. RNA Extraction and DNase Digestion.....	35

C. UV Spectrophotometer Quantification of RNA.....	38
D. Fluorescent mRNA Differential Display.....	39
E. Polyacrylamide Gel Extraction.....	44
F. PCR Amplification and Purification of DD Products.....	44
G. Cloning of DD Products into pUC19 Cloning Vector.....	45
VII. RESULTS.....	49
A. RNA Isolation.....	49
B. UV Spectrophotometer Quantification.....	50
C. Differential Display.....	50
D. PCR-Agarose Purification.....	54
VIII. DISCUSSION.....	56
IX. REFERENCES.....	59

LIST OF FIGURES

1. Figure 1: CMT Related Peripheral Neuropathy in Legs.....	14
2. Figure 2: CMT Related Peripheral Neuropathy in Foot.....	14
3. Figure 3: CMT Related Peripheral Neuropathy in Hands.....	14
4. Figure 4: Normal Nerve with Intact Myelin Sheath.....	16
5. Figure 5: Diseased Nerve with Damaged Myelin Sheath.....	16
6. Figure 6: Electron Micrograph of Sural Nerve Biopsy.....	18
7. Figure 7: Mechanism of CMT Type 1A Duplication.....	21
8. Figure 8: Proposed Protein Structure of PMP22.....	26
9. Figure 9: Protein Structural Organization of the Cochlear Duct.....	29
10. Figure 10: Immunocytochemistry of Mouse Cochlea with Antibody Directed Against Murine PMP22.....	31
11. Figure 11: Flow Chart of Methods.....	34
12. Figure 12: Replication, Transcription, and Translation of Genetic Material.....	36
13. Figure 13: RNA Loaded on a 1% Agarose Gel.....	37
14. Figure 14: Schematic Diagram of Differential Display Methodology.....	39
15. Figure 15: Wild Type and Trembler-J Differentially Displayed Transcripts.....	43
16. Figure 16: pUC19 Plasmid DNA with Insert.....	46
17. Figure 17: Evaluation of RNA Integrity by Agarose Gel Electrophoresis...	49

18. Figure 18: Denaturing Acrylamide Gel Featuring H-TG Anchor Primer and Arbitrary Primer 4 PCR Products.....	51
19. Figure 19: H-TA PCR Products Showing No Differentially Displayed Transcripts.....	54
20. Figure 20: Agarose Gel Showing PCR Products of Differentially Displayed Transcripts.....	54

LIST OF TABLES

1. Table 1: Clinical Features of Charcot-Marie-Tooth.....	19
2. Table 2: Genetic Heterogeneity of Charcot-Marie-Tooth.....	20
3. Table 3: RNA Concentration and A260/A280 Ratio of RNA Samples.....	50
4. Table 4: DD Bands Resulting from Anchor/Arbitrary Primer Combinations.....	52
5. Table 5: Primer Combinations Producing Down Regulation in Trembler-J PCR Products.....	53
6. Table 6: Primer Combinations Producing Up Regulation in Trembler-J PCR Products.....	53

INTRODUCTION

Charcot-Marie-Tooth (CMT) is the most common form of inherited peripheral neuropathy. It is characterized by degeneration of the peripheral nerves, resulting in distal muscle atrophy, sensory loss, and deformities of the hands and feet (Charcot and Marie, 1886; Tooth, 1886). This study focuses on a genetic variant of CMT that is associated with a profound and progressive form of hereditary deafness. Genetic and haplotype analysis mapped this form of CMT to chromosome 17p11.2-p12 (Kovach et al., 1999). Molecular analysis identified a point mutation in the PMP22 gene that maps within this region (Kovach et al., 1999). Thus, the protein encoded by the PMP22 gene (peripheral myelin protein) is a component of the nervous system where it is predicted to assist in the formation and maintenance of myelin sheaths surrounding nerve fibers. PMP22 protein is also found in non-neural tissues, particularly those of the epithelium, lung, and intestine. PMP22 expression has been proposed to have two functions: a role in peripheral nerve myelination and a role in cell growth regulation in non-neural tissues. The purpose of this study is to examine the role of PMP22 in non-neural tissues during development. Information gathered about the general function of PMP22 will be used to further understand the role of PMP22 in the non-neural aspect of hearing development.

Review of Hereditary Neuropathies

The nervous system is organized into the central nervous system (CNS), consisting of the brain and spinal cord, and the peripheral nervous system (PNS), consisting of nerve fibers that carry information between the CNS and the periphery (Sherwood, 2004). Hereditary neuropathies are a group of inherited disorders of the PNS. There are four main classifications of hereditary neuropathy based on clinical symptoms and focal lesion: (1) hereditary motor and sensory neuropathy, (2) hereditary sensory neuropathy, (3) hereditary sensory and autonomic neuropathy, and (4) hereditary motor neuropathy (Dyck and Ohta, 1975). Hereditary motor and sensory neuropathy (HMSN) is the largest class of peripheral neuropathies and involves both motor and sensory nerves (Dyck and Ohta, 1975). This class can be further subdivided based on neuropathology into HMSN type I and HMSN type II (Dyck and Ohta, 1974). HMSN type I exhibits primarily demyelination and nerve hypertrophy with little axonal involvement whereas HMSN type II is nondemyelinating with primarily axonal pathology (Dyck and Ohta, 1975). Hereditary sensory neuropathy (HSN) is distinguished from HMSN in that disease pathology is associated with only sensory nerves (Dyck and Ohta, 1975). Hereditary sensory and autonomic neuropathy (HSAN) is similar to HSN except that it affects sensory nerves in addition to the involuntary processes of the autonomic nervous system (Dyck and Ohta, 1975).

Hereditary motor neuropathy (NMN) is exclusively a motor disorder of the PNS (Dyck and Ohta, 1975).

Symptoms of the four classes of hereditary neuropathies are overlapping and may include numbness and tingling of feet and hands, muscle weakness, particularly of distal muscles, and sclerosis. Charcot-Marie-Tooth is a hereditary motor and sensory neuropathy (HMSN) and accounts for the majority of hereditary neuropathies.

Charcot-Marie-Tooth (CMT)

Charcot-Marie-Tooth disease is the most common genetic neuropathy with an incidence of 1 in 2500 (Skre, 1974). The disease is named for the three physicians who first identified it in 1886: Jean-Martin Charcot, Pierre Marie, and Howard Henry Tooth. Charcot-Marie-Tooth is characterized by degeneration of peripheral nerves, resulting in distal muscle atrophy, sensory loss, and deformities of the hands and feet (Figures 1, 2, 3) (Charcot and Marie, 1886; Tooth, 1886). The severity of symptoms, however, is variable among patients and even family members with the disease (Kaku et al., 1993). Progression of CMT is gradual, and onset of symptoms occurs most often in adolescence or early adulthood (Garcia et al., 1995 and Lupski et al., 1991). Presentation, however, can be delayed until mid-adulthood (Garcia et al., 1995 and Lupski et al., 1991).

Physical Characteristics of CMT



Figure 1: *CMT Related Peripheral Neuropathy in Legs.* Atrophy in the leg muscles results from CMT related peripheral neuropathy. This causes the lower legs take on an inverted appearance due to the loss of muscle bulk.



Figure 2: *CMT Related Peripheral Neuropathy in Feet.* The small muscles of the feet are weakened from nerve degeneration due to CMT. This results in high arches and hammertoes. Weakened dorsiflexor muscles cause patients frequently trip over small objects.



Figure 3: *CMT Related Peripheral Neuropathy in Hands.* Muscle atrophy due to nerve degeneration occurs in the hands and causes difficulty in performing fine motor skill tasks. In severe cases, claw hand deformities can be seen.

Patients suffering from Charcot-Marie-Tooth often have deformities of the legs, hands, and feet as a result of peripheral neuropathy. CMT is characterized by slowly progressive weakness of the distal limb muscles (Garcia et al., 1995 and Lupski et al., 1991). Muscle weakness begins in the feet and legs (Murakami et al., 1996) (Figures 1 and 2). As a result of weakness of the dorsiflexor muscles of the feet, patients frequently trip and sprain their ankles (Murakami et al., 1996). Also, the foot drops with each step and forces the patient to lift the knee, giving the “steppage” gait (Murakami et al., 1996). Atrophy of the leg muscles gives the inverted champagne bottle appearance and is prominent in slender and severely

affected patients (Murakami et al., 1996). Patients commonly complain of leg cramps after long walks and poor tolerance to cold weather due to loss of muscle mass (Murakami et al., 1996). Weakness of the intrinsic hand muscles usually occurs late in the course of the disease but may not be related to the degree of leg weakness or atrophy (Murakami et al., 1996). Patients frequently complain of difficulty in manipulating small objects that require fine finger movements and approximation of the thumb with other fingers (Murakami et al., 1996) (Figure 3). In severe cases, claw hand deformities may be seen (Murakami et al., 1996).

Causes of CMT

CMT is a hereditary disease of the peripheral nervous system. In order to understand the pathophysiology and progression of CMT, one must have an understanding of the peripheral nervous system, its components, and how they function in the human body. A nerve cell communicates information to distant targets in the peripheral nervous system by sending electrical signals down a long, thin part of the cell called an axon (Sherwood, 2004). In order to increase the speed at which these electrical signals travel, the axon is insulated by myelin, which is produced by another type of cell called the Schwann cell (Sherwood, 2004). Myelin twists around the axon and prevents dissipation of the electrical signals (Figure 4) (Sherwood, 2004). Without an intact axon and myelin sheath, peripheral nerve cells are unable to activate

target muscles or relay sensory information from the limbs back to the brain (Figure 5) (Sherwood, 2004).

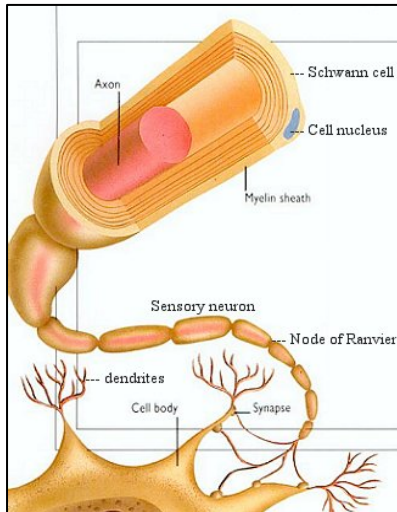


Figure 4: Normal Nerve with Intact Myelin Sheath. Schwann cells produce myelin. CMT type 1 affects Schwann cell formation leading to an exposed axon.

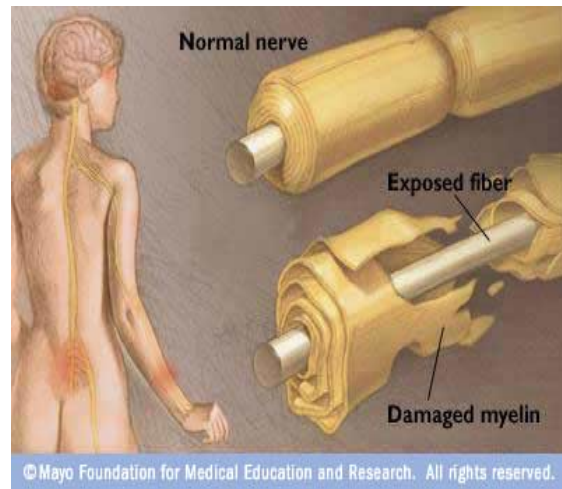


Figure 5: Diseased Nerve with Damaged Myelin Sheath. Because of myelin damage, sensory information is not transmitted normally. As a result, patients suffering from CMT experience sensory loss.

CMT is caused by mutations in genes that produce proteins involved in the structure and function of either the peripheral nerve axon or the myelin sheath (Sherwood, 2004). Although different proteins are affected in the various forms of CMT disease, all of the mutations affect the normal function of the peripheral nerves (Sherwood, 2004). Consequently, these nerves slowly degenerate and lose the ability to communicate with their distant targets (Sherwood, 2004). The degeneration of motor nerves results in muscle weakness and atrophy in the extremities (arms, legs, hands, or feet),

and in some cases the degeneration of sensory nerves results in a reduced ability to feel heat, cold, and pain (Sherwood, 2004).

Clinical and Genetic Heterogeneity of CMT

Charcot-Marie-Tooth is a clinically (Table 1) and genetically (Table 2) heterogeneous group of disorders of the peripheral nerves also referred to as the hereditary motor and sensory neuropathies (HMSN) (Dyck et al., 1993). Two major dominant clinical types of CMT have been defined on the basis of electrophysiological studies; CMT type 1 and CMT type 2 (Table 1) (Lupski et al. 1991; Dyck et al. 1993).

CMT1 is characterized by uniformly decreased nerve conduction velocities and nerve demyelination. The median nerve conduction velocities in patients with CMT1 usually are less than 42 m/sec (Dyck and Lambert, 1968). In addition to being decreased and uniform, the nerve conduction velocities of CMT1 are also symmetric and bilaterally distributed from ipsilateral nerves and between proximal and distal nerve segments, suggesting that primarily Schwann cells are affected (Kaku et al., 1993; Uncini et al., 1995).

Peripheral biopsies from patients with CMT1 show a neuropathology characterized by decreased number of myelinated fibers and hypertrophic changes due to onion bulb formations (Figure 6). These onion bulb structures consist of circumferentially directed Schwann cells and their processes around myelinated and demyelinated internodes (Griffin, 1995; Lupski and Garcia, 1992).

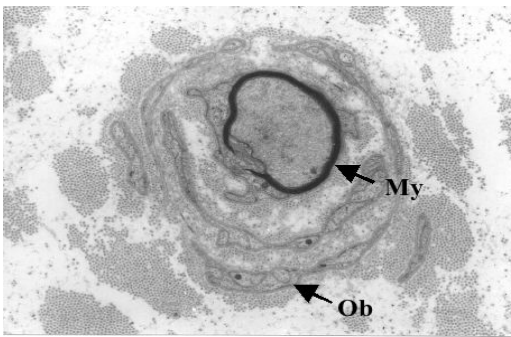


Figure 6: *Electron Micrograph of Sural Nerve Biopsy.* This picture shows thinly myelinated axons, enlargement of the peripheral nerve, and onion bulb whirls (Schwann cell hypertrophy). Abnormal Schwann cells are characteristic of CMT type 1.

Ob = onion bulb whirls
My = myelin

In contrast to CMT type 1, CMT type 2 displays normal to near-normal nerve conduction velocities (>38 m/s), associated with a neuronal (axon) defect (Harding and Thomas, 1980). For differential diagnosis, a motor nerve conduction velocity value of 38 m/sec in the median nerve is often used as the division to separate CMT1 from CMT2 (Harding and Thomas, 1980).

Two other major types of CMT are X-linked CMT (CMTX) and CMT type 4 (Dyck et al., 1993). CMTX is similar to CMT1 clinically and neuropathologically. Male patients with CMTX, however, are more severely affected than female patients since females carry two copies of the X-chromosome in contrast to the one copy carried by males. Affected females that have one normal X-chromosome will have a milder form of the disease than affected females with mutations on both X-chromosomes. In electrophysiologic studies of known CMTX families, affected men have slow motor nerve conduction velocities (<40 m/sec), whereas affected or carrier females exhibit intermediate motor nerve conduction velocities (>40m/sec) (Nicholson and Nash 1993). CMT type 4 is an autosomal recessive form of the disease. It is rare and results in hypomyelination. The various clinical features of the major CMT types are shown in Table 1 below.

Table 1: Clinical Features of Charcot-Marie-Tooth

Type	Age of Onset	Early Symptoms	Motor NCVs	Pathological Features
CMT1	First two decades of life.	Distal leg muscle weakness.	Slowed	Decreased number of myelinated fibers, onion bulbs.
CMT2	Usually the first two decades of life, up to the seventh decade.	Distal leg muscle weakness.	Normal	Decreased number of large myelinated fibers.
CMTX	First two decades of life.	Distal leg muscle weakness.	Slowed	Decreased number of myelinated fibers, onion bulbs.
CMT4	First decade of life.	Distal muscle weakness.	Severely slowed.	Hypomyelination

At least twenty five different genetic variants of CMT have been described and include autosomal dominant, autosomal recessive, and X-linked forms. Table 2 describes the various types, inheritance patterns, chromosome locations (locus), and associated genes of Charcot-Marie-Tooth disease.

Table 2: Genetic Heterogeneity of Charcot-Marie-Tooth Disease.

Type	Inheritance	Locus	Gene
CMT1A	AD	17p11.2-p12	PMP22
CMT1B	AD	1q21.2-q23	MPZ
CMT1C	AD	16p13.1-p12.3	LITAF/SIMPLE
CMT1D	AD	10q21	ERG2
CMT1E	AD	1p22	---
CMT1F	AD	8p21	---
CMT2A1	AD	1p35-p36	KIF1B
CMT2A2	AD	1p36	MFN2
CMT2B	AD	3q13-q22	RAB7
CMT2C	AD	12q23-q24	---
CMT2D	AD	7p14	GARS
CMT2E	AD	8p21	---
CMT2F	AD	7q11-q21	HSPB1
CMT2G	AD	12q12	---
CMT2I	AD	1q22	---
CMT2J	AD	1q22	---
CMT2L	AD	12q24	HSPB8
CMT4A	AR	8q13-q21.1	---
CMT4B	AR	11q23	MTMR2
CMT4B2	AR	11p15	SBF2
CMT4C	AR	5q32	SH3TC2
CMT4D	AR	8q24	NDRG1
CMT4E	AR	10q21	ERG2
CMT4F	AR	19q13	---
CMTX	X-linked	Xq13	---

AD = Autosomal Dominant **AR** = Autosomal Recessive

The most common type of CMT is CMT1A which accounts for more than seventy percent of CMT cases (McKusick, 1992). A 1.5 Mb DNA duplication of chromosome 17p11.2-p12 is observed in most patients with CMT type 1A (Figure 7) (Lupski et al., 1991; Pentao et al., 1992; Raeymaekers et al., 1991).

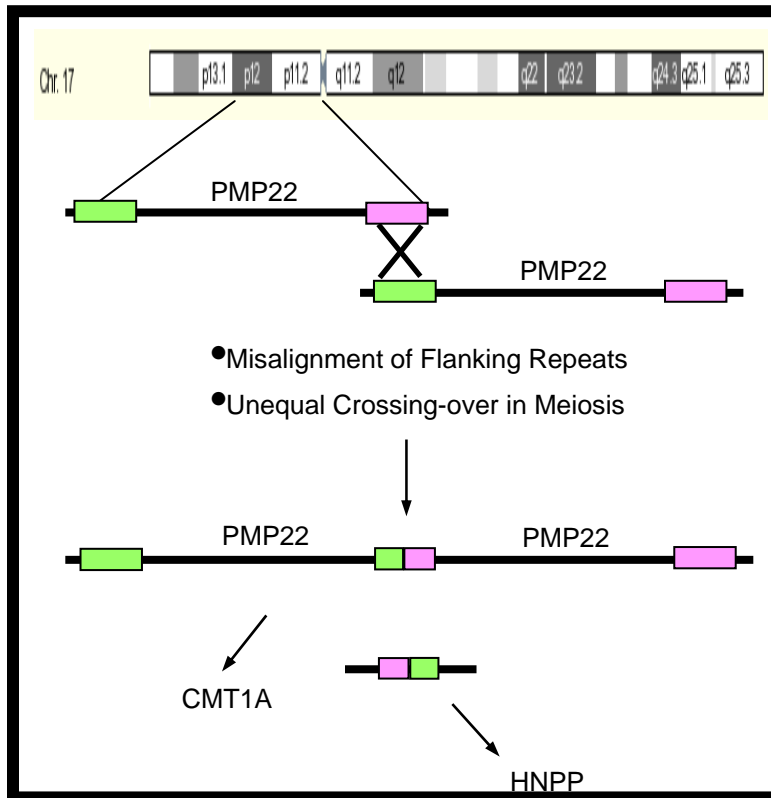


Figure 7: Mechanism of CMT type 1A Duplication. The region of Chromosome 17p11.2-12 containing the *PMP22* gene is flanked by repeat sequences (green and pink boxes). During meiosis I, misalignment of the repeat elements of homologous chromosomes can lead to unequal crossing-over. The result is a duplication of the *PMP22* gene on one chromosome and a reciprocal deletion of the *PMP22* gene on the other chromosome. Inheritance of the *PMP22* duplication causes CMT1A, whereas individuals inheriting the deletion have a related neuropathy known as Hereditary Neuropathy with liability to Pressure Palsy (HNPP).

Overexpression of a gene for CMT1A, peripheral myelin protein-22 (PMP22), which maps within the duplication and encodes a myelin-specific protein, has been implicated in the majority of individuals with this disorder (Roa and Lupski, 1993). The object of this study is to examine the molecular pathophysiology of a genetic variant of CMT type 1 associated with progressive hearing loss.

Diagnosis of CMT

Diagnosis of CMT is complex and multifaceted. A standard patient history is combined with a family medical history and neurological exam to accurately diagnose CMT. During the neurological examination, a physician will look for evidence of muscle weakness in the arms, legs, hands, and feet, decreased muscle bulk, reduced tendon reflexes, and sensory loss (Sabir and Lyttle, 1983). Foot deformities, such as high arches, hammertoes, inverted heel, or flat feet are also common in CMT patients (Sabir and Lyttle, 1983). Other orthopedic problems, such as mild scoliosis or hip dysplasia, may also be present (Sabir and Lyttle, 1983). A specific symptom that may be found in patients with CMT1 is nerve enlargement that may be felt or even seen through the skin. This nerve enlargement is due to the abnormally thickened myelin sheaths. Based on this knowledge of CMT pathophysiology, physicians will order electrodiagnostic tests to confirm a CMT diagnosis. This testing consists of two parts: nerve conduction studies and electromyography (EMG). Specific abnormalities in nerve conduction readings signify axon degeneration. EMG may be used in further characterizing the distribution and severity of peripheral nerve involvement.

Treatment of CMT

The clinical variability and genetic heterogeneity in CMT often poses difficult diagnostic challenges (Timmerman et al., 2006). Since no specific treatment is available, the physician provides clinical and genetic counseling and suggests symptomatic and rehabilitative treatment options (Dyck et al., 1993). Many patients live to be very old and only a few become confined to a wheelchair (Dyck et al., 1993). Most affected persons are able to work in manual labor, assembly lines, clerical work, or as professionals (Dyck et al., 1993). Symptoms are more difficult to anticipate because they may depend also on nondisease factors (Dyck et al., 1993). Younger patients with CMT may be advised to seek training in an area that does not require unusual manual dexterity or strength (Dyck et al., 1993). Because foot deformities are characteristic of CMT, properly fitting and well-made shoes are recommended for patients (Dyck et al., 1993). Foot surgery to correct for excessively inverted feet or severe degrees of pes cavus and hammertoes may improve walking and alleviate pain over pressure points and prevent plantar ulcers (Dyck et al., 1993). More research in the molecular aspect of CMT is needed to find a cure or truly effective treatment. A better understanding of the molecular architecture of the peripheral nerve, the functional pathways, the myelination process, and the complex interaction between myelinating Schwann cells, the axon, and muscle is crucial to identify targets for therapeutic interventions (Timmerman et al., 2006).

Genetics of Deafness

Hereditary hearing loss is divided into two categories, syndromic and non-syndromic. Seventy percent of hereditary deafness cases are nonsyndromic, where the ear is the only system affected (Cohen et al., 1995). Typically, in nonsyndromic hearing loss deafness is the only detectable symptom; however, in some cases malfunction of the vestibular system also occurs (Robertson and Morton, 1999). In addition to having hearing loss, individuals may also experience difficulty with balance and other equilibrium issues.

Over 40 chromosomal loci have been identified for nonsyndromic hearing loss through linkage studies (Morton, 1991). Nonsyndromic hereditary hearing loss can be subdivided into three categories, autosomal dominant, autosomal recessive, and X-linked. Perturbations of equilibrium are harder to ascertain in humans due to the compensatory mechanisms of the visual and proprioceptive systems which contribute to overall balance maintenance (Robertson and Morton, 1999). Upon examination and specific vestibular testing, some individuals with hearing loss also show vestibular pathology (Robertson and Morton, 1999). In mice, this correlation has been more obvious, because most mouse strains with hearing defects are identified on the basis of an abnormal behavior have been given names such as shaker, twirler, waltzer, and trembler (Robertson and Morton, 1999).

CMT and Deafness

CMT is not normally associated with deafness, but co-presentation of CMT and deafness has been found in several autosomal dominant families. De Weerd and Heerspink (1974) were the first to report autosomal dominant neuropathy and hearing loss in a large family. Onset of hearing loss began in early thirties and forties and progressed slowly. Hamiel et al. (1993) reported a family from Israel with CMT and sensorineural deafness. Onset of deafness occurred in infancy and early childhood. Kouseff et al. (1982) described a large central Illinois family with autosomal dominant CMT and deafness. Onset occurred in childhood with weakness of the peroneal muscles, followed by atrophy, pes calcaneovarus (dorsoflexion and inversion of foot), steppage gait, poor balance, diminished sensation in the legs, hammer toes, pes cavus (high arched foot), claw hands, and absent deep tendon reflexes (Kouseff et al., 1982). While there have been several reports describing the co-presentation of CMT and deafness, there has been very little written on the molecular nature of this hearing loss.

This study began with the genetic analysis of 70 members from the central Illinois family described by Kouseff (1982). Haplotype and DNA sequencing analysis identified a unique point mutation (Kovach et al., 1999) in the PMP22 gene rather than the 1.5Mb duplication normally associated with CMT1A. This point mutation causes a guanine (purine) to cytosine (pyrimidine) transversion in the third coding exon resulting in an Ala67Pro

substitution in the second transmembrane domain of PMP22 (Kovach et al, 1999). Interestingly, audiological studies of this family revealed both a neural and cochlear (non-neural) component to hearing loss. This observation is consistent with a dual role of PMP22 in both neural and non-neural tissues. To gain an understanding of the role of PMP22 in non-neural tissue, this study will examine PMP22 expression in a mouse model for CMT at one time point during development. This study will identify a subset of genes differentially regulated by PMP22 in a mutant mouse as compared to a normal mouse. Examination the effects of PMP22 on gene interactions at different developmental time points may shed light on the structural and functional aspects of cochlear development and normal hearing.

Peripheral Myelin Protein (PMP22)

Peripheral myelin protein 22 (PMP22) is a hydrophobic 22kDa glycoprotein.

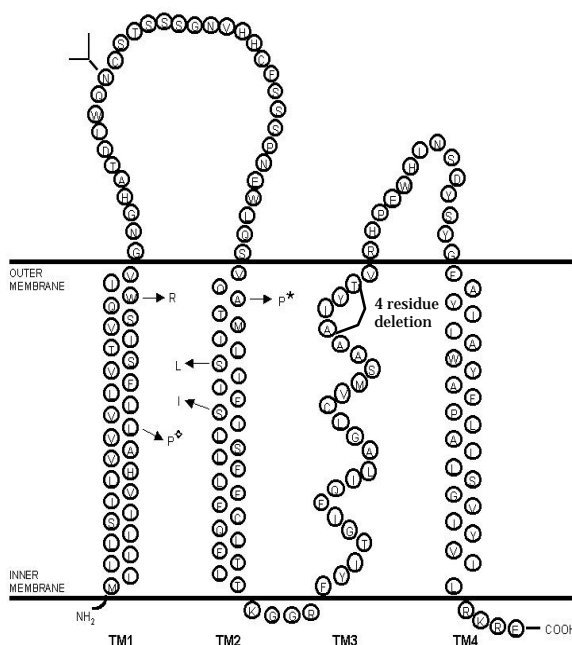


Figure 8: Proposed Protein Structure of PMP22. Mutations in which deafness have been described in addition to CMT are presented with arrows indicating the amino acid substitution. The unique substitution associated with CMT and deafness in our Central Illinois family (Ala67Pro) is designated with an asterisk (*). The Trembler-J mutation (Leu16Pro) is designated with a diamond (◊).

It is mainly expressed by myelinating Schwann cells where it is incorporated into compact myelin (Welcher et al., 1991; Snipes et al., 1992; Naef and Suter, 1998). Its proposed structural model predicts four transmembrane domains and two extracellular loops (Figure 8). Interestingly, the proposed structure of PMP22 bears a striking similarity to that of the connexins, three of which (GJB2, GJB3, and GJB6) are responsible for the nonsyndromic forms of deafness DFNB1, DFNA2, and DFNA3, respectively (Kovach et al., 1999).

PMP22 makes up 1-5% of total peripheral nervous system myelin protein and is of crucial importance in myelin formation and maintenance (Suter and Snipes, 1995; Suter and Nave, 1999). Missense mutations in the PMP22 protein and aberrant PMP22-gene dosage have been linked to various hereditary motor and sensory neuropathies (Suter and Snipes, 1995; Suter and Nave, 1999). Although the highest expression levels are found in myelin-forming Schwann cells, PMP22 mRNA can be detected in several developing and mature non neural tissues (Baechner et al., 1995; Taylor et al., 1995; Wulf and Suter, 1999). This evidence suggests that PMP22 may have a more general function besides its role in the development and maintenance of myelin.

Correlative evidence and gene transfer experiments *in vitro* suggest a possible role for PMP22 and other members of the gene family in the regulation of cell cycle, cell proliferation, apoptosis, and cell spreading

(Fabbretti et al., 1995; Marvin et al., 1995; Taylor et al., 1995; Zoidl et al., 1995; Ben-Porath et al., 1998; Brancolini et al., 1999, Attardi et al., 2000).

Figure 8 shows the mutations in which deafness have been described in addition to CMT. The unique substitution associated with CMT and deafness in the central Illinois family studied by Kovach (1999) is designated with an asterisk. All individuals carrying this mutation display profound, sensorineural hearing loss in addition to CMT. This mutation results in the alteration of an alanine residue containing an aliphatic hydrocarbon group at position 67 to a proline residue containing an aliphatic cyclic structure. The mutation is predicted to disrupt the B-sheet structure of the second transmembrane domain and perhaps affect membrane integration and extracellular interactions of PMP22.

Growth Arrest Specific (gas) Genes

The murine *PMP22* gene (Figure 8), also designated *gas 3*, was originally isolated as a growth arrest specific (gas) gene (Manfioletti et al., 1990; Welcher et al., 1991). The family of *gas* genes that includes *PMP22* has a characteristic pattern of expression in non-neural tissues. Expression is induced during periods of growth arrest and down regulated at terminal differentiation (Coccia et al., 1992). In contrast, *PMP22* expression in cultured Schwann cells is not affected by growth arrest. It has been proposed that *gas* genes play a role during the intervening period where cells committed to a particular lineage continue to divide at a reduced rate. Not surprisingly,

gas genes have been shown to regulate gene expression (Ron and Habener, 1992), apoptosis (Fabretti et al., 1995) and timing of cell division (Zoidl et al., 1995).

Trembler-J mice as a Model for CMT1A

The spontaneous mutants Trembler (Tr) and Trembler-J (Tr-J) carry point mutations in the PMP22 gene and represent animal models for severe forms of Charcot-Marie-Tooth Syndrome. The mutations are autosomal dominant and result in an unsteady gait, tremor, and quadriparesis in clinically affected animals. The Trembler mutation leads to the non-conservative glycine to aspartic acid substitution at amino acid position 150 of the PMP22 protein, whereas the Trembler-J mutation results in replacement of proline for lysine at codon 16 (Suter et al., 1992).

Patients heterozygous for mutations identical to Trembler and Trembler-J have been described (Valentijn et al., 1992; Ionasescu et al., 1997). Affected individuals present with classical neurological symptoms and nerve pathology of CMT type 1A. The peripheral auditory system has been evaluated in adult mice heterozygous for the Tr-J mutation (Zhou et al., 1995) and suggests audiological dysfunction associated with PMP22 mutations. The structural organization of the cochlear duct is presented in Figure 9.

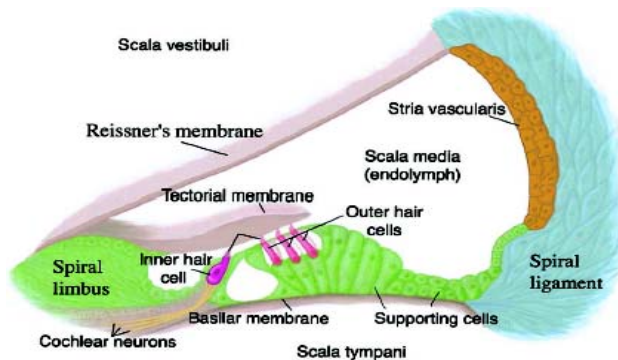


Figure 9. Structural Organization of the Cochlear Duct (Resendes et al., 2001). The PMP22 protein localized primarily to the stria vascularis. It is proposed to function in maintaining electrochemical potential of the endolymph.

Figure 10 presents PMP22 immunolocalization images from cochlea of control and Trembler-J heterozygous experimental mice (Kovach et al., unpublished). Intense staining of the cochlear nerve, an internal positive control, is observed in all cochlea, but the staining pattern in mutant mice is more diffuse and less pronounced than seen in the control cochlea nerve. This is consistent with previous studies that suggest aberrant trafficking of the PMP22 protein in Trembler-J mice (Tobler et al., 1999). The Trembler-J mouse has been chosen for this study because of the preliminary histological examinations of the inner ear and auditory system suggest hearing impairment in these mice (Zhou et al., 1995).

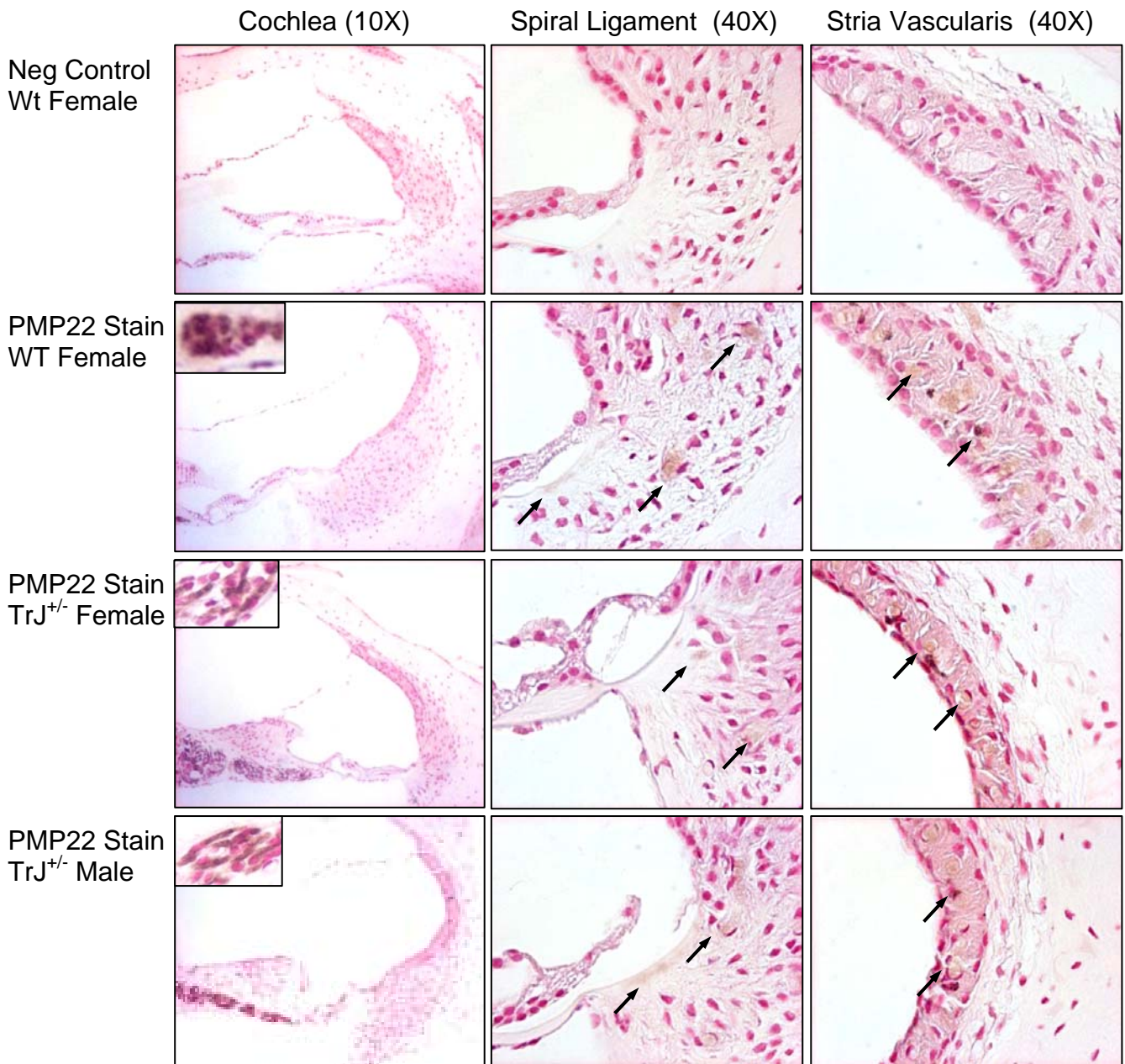


Figure 10. Immunocytochemistry of Mouse Cochlea with Antibody Directed Against Murine PMP22 Protein.

Cellular localization of the PMP22 protein is demonstrated in cochlea of 6-week old C57BL/6J (wild type control) and C57BL/6J-Pmp22^{Tr-J/+} (heterozygous mutant) mice. (Kovach et al., unpublished)

Row 1: Immunocytochemistry of wildtype C57BL/6J mouse cochlea without application of primary α -PMP22 antibody (Negative control)

Row 2: Anti-PMP22 immunocytochemistry of wildtype C57BL/6J mouse cochlea (Positive control)

Row 3: Anti-PMP22 immunocytochemistry of C57BL/6J-Pmp22^{Tr-J/+} cochlea from female mouse (Experimental)

Row 4: Anti-PMP22 immunocytochemistry of C57BL/6J-Pmp22^{Tr-J/+} cochlea from male mouse (Experimental)

The insets in column I, rows 2, 3 and 4 are magnifications (40X) of the spiral ganglia of the cochlear nerve from these tissues, showing intense neural staining of accessory Schwann cells with α -PMP22 antibody. Arrows indicate areas of PMP22 localization in non-neural tissues of the cochlea, specifically the stria vascularis and spiral ligament.

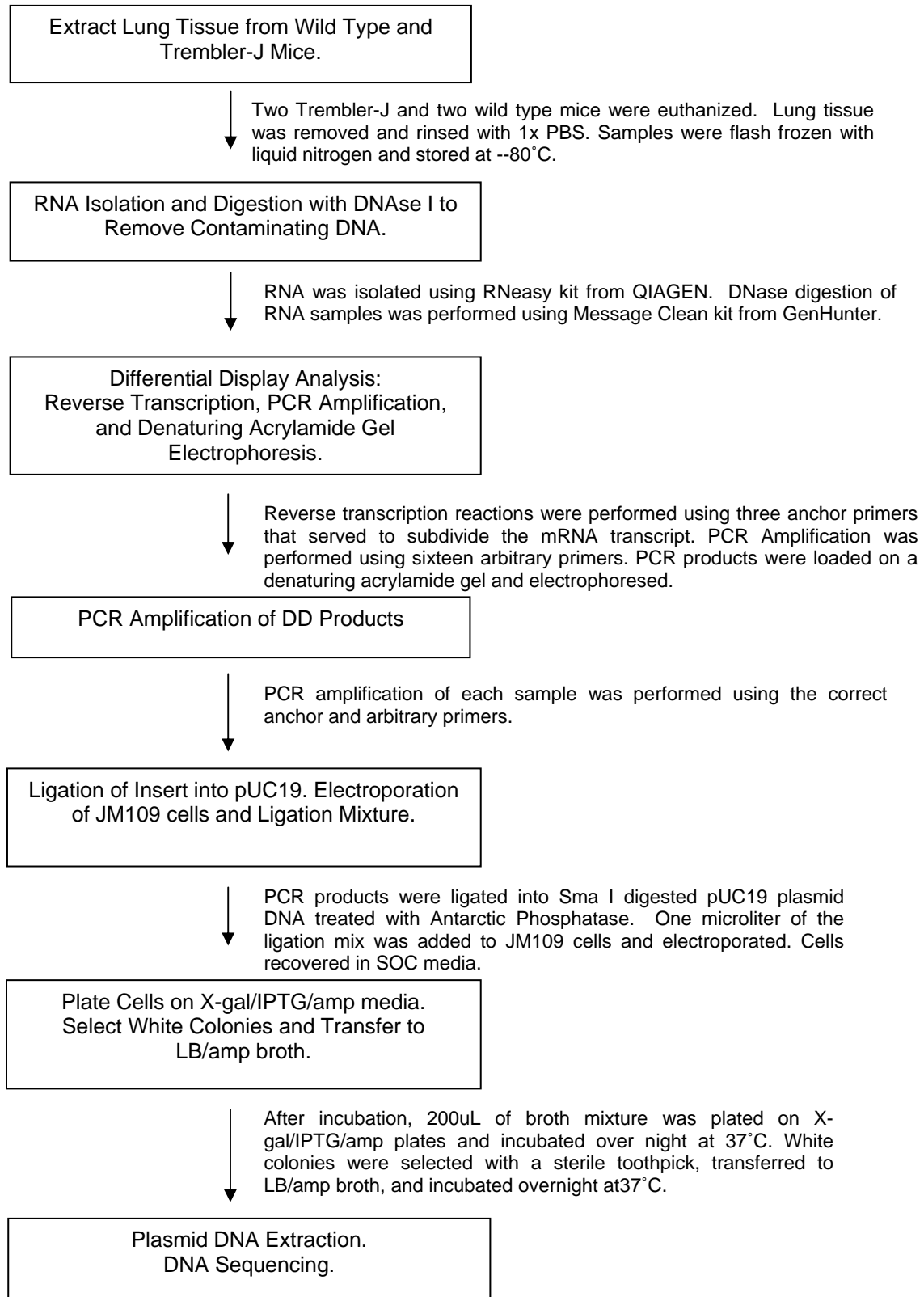
To explain the cochlear component of the hearing loss, it is likely that sensory cells would also stain with PMP22 because they are the primary receptor cells, responsible for transducing the vibrational energy of sound into electrical charges. However, non-neural staining of PMP22 is observed primarily in the marginal and intermediary cells of the stria vascularis (Figure 10). This suggests that PMP22 may function in maintaining the electrochemical potential of the endolymph (refer to Figure 9). Weak, occasional localization of the PMP22 protein is observed in cells of spiral ligament and basilar membrane. Overall, neural and non-neural staining in Tr-J mice is reduced when compared to the staining pattern of wild type mice. Heterozygous mice are used for the affected samples because the phenotype of heterozygous mice is much milder than that of the homozygous mice, thus demonstrating that PMP22 is a dosage-sensitive myelin component (Adlkofer et al., 1995). In this study, the Trembler-J mouse model will be used to examine the role of PMP22 in gene expression in non-neural tissue.

Purpose of Project

The purpose of this project is to identify genes influenced by PMP22 expression in non-neural tissues at developmental time points. Comparative analysis of control and experimental groups should aid in the understanding of PMP22 function and its interaction with other genes and gene products. A general understanding of PMP22 interaction during the development of non-neural tissues will most likely shed light on its specific influence of inner ear development and its role in normal hearing. This project specifically examined the influence of PMP22 on gene expression in the lung tissue of wild type and Trembler-J mice at the 21 days post delivery time point. Differential display technology allowed differences in gene expression to be shown. Up-regulated and down-regulated transcripts were excised and amplified. Cloning of differentially displayed transcripts will allow the DNA sequencing of individual transcripts. Identified genes will be grouped according to structure and function in order to examine PMP22 gene interaction during the development of non-neural tissues.

MATERIALS AND METHODS

Figure 11: *Flow Chart of Methods*



Plasmid DNA was extracted using a miniprep procedure.

Trembler J Mouse Model and Animal Care and Use

Two 21 day old wild type (non mutant) and two 21 day old heterozygous Trembler-J (TrJ) mice were chosen for this study to compare PMP22 gene expression levels in a mouse model for Charcot-Marie-Tooth disease. Approval for this animal protocol was obtained from the University of Tennessee at Chattanooga Institutional Animal Use and Care Committee (protocol # 1005MJK-02).

Mice were individually euthanized by anesthetic overdose via halothane inhalation (0.2 mL in a closed container / 2 weeks). Prior to tissue dissection and harvest, the mouse's external surface was rinsed with 70% ethanol. After decapitation, the cochlea, lungs, intestines, kidneys, heart, and sciatic nerve were dissected and rinsed with cold 1x PBS. Tissues were quickly transferred to separate cryogenic tubes and flash frozen using liquid nitrogen. Labeled tubes were stored at -80°C for approximately two weeks until RNA extraction.

RNA Extraction and DNase Digestion

To evaluate gene expression patterns in control (wild type) and experimental (Trembler-J) samples, RNA is extracted under RNase free conditions from non-neural tissue of the lung and subjected to Differential Display analysis. While DNA is the primary source of genetic information, it does not directly serve as the template used to direct protein synthesis (Figure 12). The information in DNA is copied into messenger RNA (mRNA) during

transcription. The mRNA is then translated into amino acids which compose a functional protein. Thus, mRNA levels reflect the levels of actively expressed gene sequences.

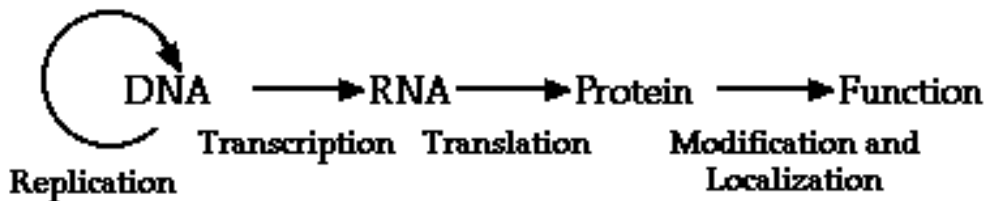


Figure 12: Replication, Transcription, and Translation of Genetic Material. DNA is converted to RNA during transcription. The RNA transcript is then translated to a functional protein. RNA can be converted to single stranded copy-DNA (cDNA) by a reverse transcription reaction. (Stanford.edu, 2007)

RNA was extracted from the lung tissue of each mouse using the QIAGEN RNeasy Mini Kit according to the manufacturer's instructions (QIAGEN, 2001). The QIAGEN RNeasy system relies on spin columns to capture and elute RNA. Tissues were removed from the -80°C freezer and immediately placed in Buffer RLT, a guanidine isothiocyanate (GITC) containing buffer, which immediately inactivated RNases. The tissues were disrupted using rotor homogenization. Ethanol was added to facilitate appropriate binding conditions. The lysate was applied to the RNeasy spin columns. Negatively charged RNA binds to the positively charged membrane of the spin column while other contaminants are washed away by Buffers RW1 and RPE, which removed proteins and excess salt, respectively. RNA was eluted from spin columns using two 30uL portions of RNase-free water.

Genomic DNA was removed from RNA samples using the MessageClean Kit according to the manufacturer's instructions (GenHunter, 2005). DNase digestion ensured that Differential Display results would not be contaminated by residual genomic DNA. Since Differential Display technology compares only the expressed portion of the genome, genomic DNA would contaminate the resulting transcript. Each DNase digestion proceeded for 60 minutes at 37°C. Included in a 1X DNase I reaction are 50µL mRNA, 5.7µL 10x reaction buffer (10mM Tris-Cl, pH 8.4, 50mM KCl, 1.5mM MgCl₂, and 0.001% gelatin), and 1.0uL DNase I enzyme. Four microliters of DNase digested RNA was loaded on an ethidium bromide stained 1% agarose gel to check for RNA integrity, as determined by the presence of 28S and 18S ribosomal RNA (rRNA) bands (Figure 13).

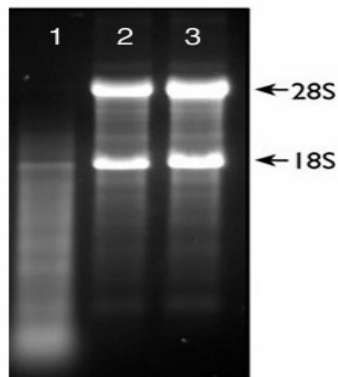


Figure 13: RNA Loaded on a 1% Agarose Gel. Lanes 2 and 3 show intact RNA with bands at 28S and 18S rRNA. Lane 1 shows degraded RNA. (Ambion.com, 2007)

UV Spectrophotometer Quantification of RNA

UV spectrophotometry was used to quantify the concentration of RNA in each sample. The concentration of RNA was determined by measuring the absorbance at 260 nm (A_{260}) (QIAGEN, 2001). To ensure significance, A_{260} readings should be greater than 0.15 (QIAGEN, 2001). An absorbance of 1 unit at 260nm corresponds to 44 μ g of RNA per mL (QIAGEN, 2001). The ratio between absorbance values at 260 and 280 nm gives an estimate of RNA purity (QIAGEN, 2001). Pure RNA has an A_{260}/A_{280} ratio of 1.9-2.1 (QIAGEN, 2001). The spectrophotometer was calibrated using DEPC-H₂O. A 1:70 dilution was performed for quantification using DNase digested RNA and DEPC-H₂O. Readings were taken at 260.0 nm, 280.0 nm, 230.0 nm, and 330.0 nm.

Fluorescent mRNA Differential Display

Differential Display (DD) was invented in 1992 by Drs. Arthur Pardee and Peng Liang to allow rapid, accurate, and sensitive detection of altered gene expression (Science. 1992, 257:967; U.S. Patent 5,262, 311). This technology allows side by side comparison of most of the mRNAs between or among related cells. (GenHunter, 2006). Differential Display is used in this study to compare gene expression in wild type and Trembler-J mice. DD works by subjecting DNase digested RNA to a reverse transcription reaction using 3 anchor primers followed by PCR amplification with several arbitrary primers (Figure 14). Differentially expressed genes are displayed on a denaturing polyacrylamide gel.

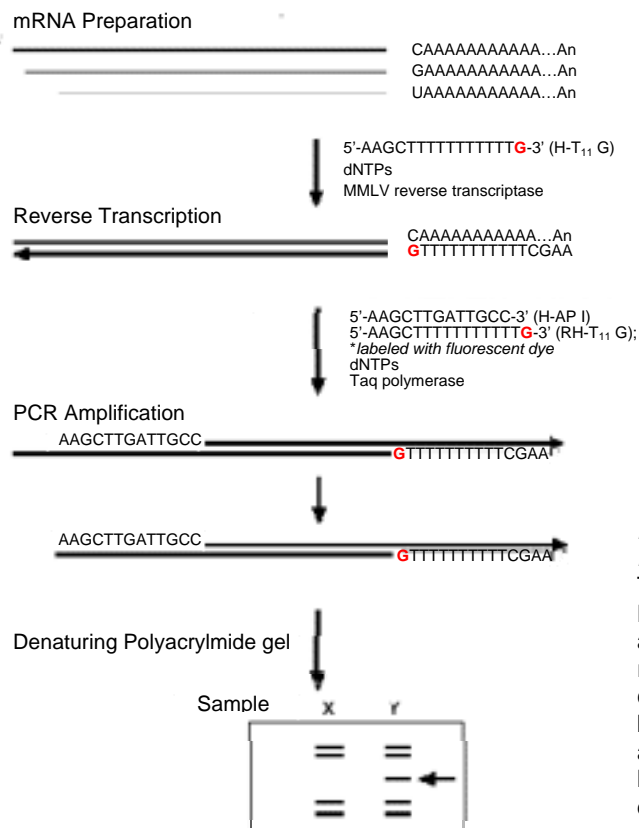


Figure 14: Schematic Diagram of Differential Display Methodology.

Three one-base anchored oligo-dT primers with 5' HindIII sites are used in combination with a series of arbitrary 13mers (also containing 5' HindIII sites) to reverse transcribe and amplify the mRNAs from a cell. Note the primer selectivity is provided by the 3' bases. The anchor primer H-T₁₁G has been used as an example. Note the 3' (G)uanine position has been highlighted in red text. PCR products are loaded on a denaturing polyacrylamide gel which shows differentially displayed bands indicated by an arrow.

Step 1: Reverse Transcription

The first step of DD is reverse transcription. Reverse transcription converts an unstable messenger RNA (mRNA) transcript to a more stable copy DNA (cDNA). Copy DNA is made from mRNA by using deoxynucleotide phosphates (dNTPs) which provide the base unit of the synthesized DNA molecule, a reverse transcription buffer to provide appropriate reaction conditions, an anchor primer that binds to the 3' end of the transcript at the poly-A tail, and an RNA dependent DNAP (DNA Polymerase) called reverse transcriptase which catalyzes the reverse transcription reaction. Reverse transcription reactions were performed on each of the four mRNA samples using three different anchor primers, H-TG, H-TC, and H-TA. Each anchor primer differs by one base (G,C, or A) and is designed to bind to the 3' end of the transcript at the poly-A tail. This serves to subdivide the mRNA transcript population. Each reaction included 9.4 μ L dH₂O, 4.0 μ L 5x RT buffer, 1.6 μ L dNTP Mix, 2.0 μ L (0.1 μ g/ μ L) total RNA (DNA-free), and 2.0 μ L M(G,C,or A) anchor primer. Master mixes were used to avoid pipetting errors. Samples were prepared in thin-walled microcentrifuge tubes and placed in a thermocycler programmed for 65 °C for 5 min → 37 °C for 60 min → 75 °C for 5 min → 4 °C soak. After 10 min at 37 °C, 1 μ L MMLV reverse transcriptase was added to each tube. Tubes were stored at -20 °C until PCR analysis.

Step 2: PCR Analysis

Polymerase Chain Reactions (PCR) were performed on each of the twelve cDNA transcript populations. PCR technology synthesizes a large amount of DNA from template DNA using primers to flank a specified locus. Each PCR reaction included template cDNA, an arbitrary primer, dNTPs which provide the base unit of the synthesized molecule, DNA polymerase (DNAP) that adds nucleotides to the 3' end, a buffer to provide correct reaction conditions for the DNAP, and the corresponding rhodamine tagged anchor primer used in the reverse transcription reaction. Taq polymerase, isolated from a thermophilic bacterium called *Thermus aquaticus*, is the DNAP used in this reaction. Each PCR reaction included 10.2 μ L dH₂O, 2.0 μ L 10X PCR buffer, 2.0 μ L H-AP primer, 2.0 μ L RH-T11M (G, C, or A) primer, 2.0 μ L cDNA, and 0.2 μ L Taq DNA polymerase. A master mix was used to minimize pipetting errors. Reagents were placed in thin walled PCR tubes to ensure uniform temperature distribution, and a drop of mineral oil was added to the top of each tube to prevent condensation of reactants in cap of tube. The three general steps of a PCR reaction are denaturing of target DNA, annealing of PCR primers to DNA template, and DNA synthesis. The optimal temperature for Taq DNA polymerase activity is 72°C. Samples were placed in a thermocycler set for 95°C for 7 minutes (initial denaturing step) followed by 94°C for 30 sec. (denaturing) → 40°C for 2 min. (annealing) → 72°C for 60 sec. (DNA synthesis) for 40 cycles (exponential amplification of DNA),

followed by 72 °C for 5 min (to ensure DNA synthesis is complete) → 4 °C hold (refrigeration step until samples can be transferred from machine). Samples were stored at 4 °C until they were loaded on a denaturing polyacrylamide gel. PCR analysis was performed using sixteen arbitrary primers. Each arbitrary primer is a random sequence of thirteen nucleotides. The specificity of these 13mers is such that they have multiple targets as opposed to PCR specific primers of twenty nucleotides. The rhodamine tag in the anchor primer allows PCR samples loaded on a gel to be viewed using a fluorescence imager. In this study, arbitrary primers 1-16 were used to analyze and compare the three transcript populations (H-TG, H-TC, and H-TA) from each of the four mice (two Trembler-J and two wild type).

Step 3: Denaturing Polyacrylamide Gel

Each PCR set was analyzed using a 6% denaturing polyacrylamide gel in TBE buffer prepared according to manufacturer instructions. The electrophoretic analysis of single stranded nucleic acids such as cDNA is complicated by the secondary structures assumed by these molecules (National Diagnostics, 2005). Separation on the basis of molecular weights requires the inclusion of denaturing agents which unfold the DNA strands and remove the influence of shape on their mobility (National Diagnostics, 2005). Nucleic acids form structures stabilized by hydrogen bonds between bases. Denaturing requires disrupting these hydrogen bonds (National Diagnostics, 2005). The most commonly used DNA denaturants are urea and formamide (National Diagnostics, 2005). Each of these forms hydrogen bonds with the

DNA bases, saturating H-bond sites and preventing the formation of inter-base bonds (National Diagnostics, 2005). Both formamide and urea effectively lower the melting point of the DNA molecules, allowing the structures to fall apart at lower temperatures (National Diagnostics, 2005). Polyacrylamide gel contains both formamide and urea (National Diagnostics, 2005). Before sample loading, the gel was pre-run for 1 hour with 1x FDD loading dye. After the initial pre-run, 3.5 μ L of each sample was mixed with 2 μ L FDD loading dye. Samples were heat denatured at 80°C for 2 minutes and then stored on ice until loading. Samples were electrophoresed at 60 watts for 1.5 hours. The gel was scanned using a FMBio fluorescence imager with the 585nm filter which is specific for rhodamine fluorescence detection. Bands of interest representing up and down regulated genes as seen in Figure 15 were excised and stored for analysis.

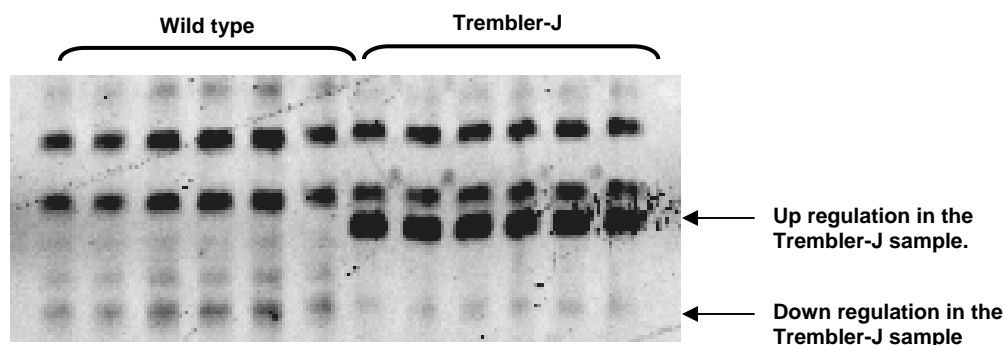


Figure 15: Wild Type and Trembler-J Differentially Displayed Transcripts. The arrows point to differentially displayed bands on a denaturing acrylamide gel. The left 6 bands represent the wild type sample, and the right 6 bands represent the Trembler-J sample. The top arrow shows up regulation in the Trembler-J sample. The bottom arrow shows down regulation in the Trembler-J sample.

Polyacrylamide Gel Extraction

In order to identify the genes differentially regulated between control and Trembler-J samples, DD products were excised from the gel and subjected to DNA extraction. The extraction was performed using the QIAquick Gel Extraction Kit according to the user-developed protocol for polyacrylamide gel extraction (QIAGEN, 2001). Each excised gel fragment (45ug) was incubated at 50 °C for one hour in 90uL of diffusion buffer (0.5M ammonium acetate; 10mM magnesium acetate; 1mM EDTA, pH8.0; 0.1% SDS). The supernatant was removed and 3 volumes of Buffer QG, a solubilization buffer specifically optimized for use with the QIAquick silica membrane, was added to the solution. The mixture was applied to a QIAquick spin column and centrifuged. Ethanol containing Buffer PE (0.75mL) was applied to the spin column to remove salts. After centrifugation, DNA was eluted from spin columns using 30µL dH₂O.

PCR Amplification and Purification of DD Products

It is essential to clone the DD products prior to DNA sequence analysis because each band on the DD gel may in actuality represent more than one transcript. PCR amplification of DD products was employed to maximize the quantity of DNA sufficient for cloning. To amplify the DNA obtained from the polyacrylamide gel extraction, a PCR amplification of each sample was performed using the corresponding anchor and arbitrary primers that were

used in the original PCR reaction. The PCR products were electrophoresed on an ethidium bromide stained 1.5% agarose gel for two hours at 125 volts. DNA bands were removed and stored for DNA extraction. DNA extraction was performed using the QIAquick Gel Extraction Kit according to the manufacturer's instructions for agarose gel extraction (QIAGEN, 2006). Isolated agarose bands (55ug) were incubated in 3 gel volumes (165uL) of buffer QG, a solubilization buffer specifically optimized for use with the QIAquick silica membrane, at 50°C for 30 minutes. One gel volume of isopropanol (to facilitate appropriate binding conditions) was added to the solution and mixed. To bind DNA, the sample was applied to the QIAquick spin column and centrifuged. To remove all traces of agarose, Buffer QG (0.5mL) was applied to the column and centrifuged. Buffer PE (0.75mL) was applied to the column to wash away salts. DNA was eluted using 30uL dH₂O. To ensure an adequate concentration of DNA for cloning, PCR-Agarose purification was performed twice.

Cloning of DD Products into pUC19 Cloning Vector

PCR-Agarose products were cloned to ensure DNA sequencing of only one transcript. pUC19 plasmid DNA was used as a cloning vector. pUC19 contains Ampicillin resistance as a selectable marker. Cloning a product into pUC19 allows for blue-white screening for inserts into the multiple cloning site (MCS). The MCS is located in the middle of the lac Z gene which encodes the enzyme B-galactosidase (B-gal). IPTG serves as an inducer for B-gal. IPTG

binds to the repressor, therefore allowing B-gal to function. The normal function of B-gal is to break down lactose into glucose and galactose. However, there are color metric substrates for B-gal such as X-gal. When X-gal is cleaved by B-gal, it forms a blue precipitate. Any cell that expresses B-gal and is grown in the presence of X-gal will be blue. An insert that has been cloned into the MCS will interrupt the Lac Z gene and therefore result in a non-functional B-gal protein (Figure 16).

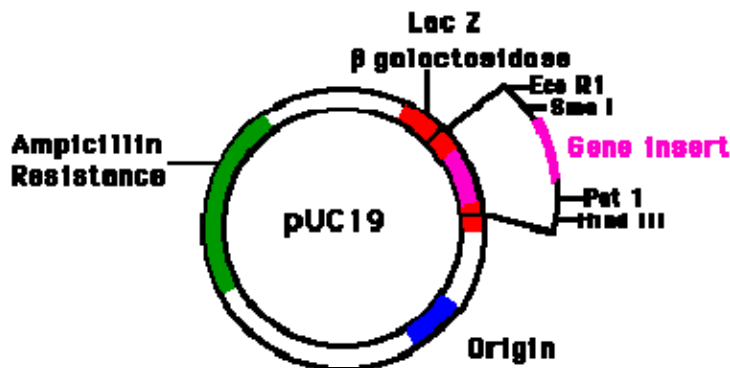


Figure 16: pUC19 Plasmid DNA with Insert.
 Differential Display products are cloned into pUC19 to ensure the DNA sequencing of only one transcript. Plasmids containing an insert will appear white because the Lac Z gene responsible for B-galactosidase expression is nonfunctional.

Since B-gal is not functional, E.coli cells transformed with pUC19 containing an insert will appear white rather than blue.

To prepare the pUC19 cloning vector for ligation of insert DNA (e.g. DD product) pUC19 was digested Sma I, a restriction endonuclease isolated from *Serratia marcescens*, according to manufacturer's instruction. Sma I digestion results in blunt end cleavage and linearization of the pUC19 plasmid, and can be heat inactivated. Digested pUC19 was then treated with

Antarctic Phosphatase to remove 5' phosphates thus preventing recircularization of the cloning vector.

PCR-Agarose purified DNA samples were ligated into Sma I digested pUC19 that had been treated with Antarctic Phosphatase. Each ligation contained 6.0 μ L purified DD product, 1.0 μ L ATP, 1.0 μ L T4 DNA Ligase, 1.0 μ L DNA Ligase buffer, and 1.0 μ L Sma I digested pUC19 treated with Antarctic Phosphatase. Reagents were combined in a thin walled PCR tube and incubated over night at 16°C overnight.

In order to clone the plasmid containing the specified insert, one μ L of the ligation mixture was added to 50 μ L of the JM109 strain of *E.coli* and electroporated to induce competence in a 2mm gap cuvette at the following setting: Voltage – 1500V, Resistor – 200 Ω , Capacitor – 25 μ F. The electroporated cells were immediately transferred to tubes containing 1mL of SOC broth in order to facilitate recovery from electroporation. The tubes were placed in a shaker and incubated at 37°C for one hour. X-gal/IPTG/amp plates were used to grow the cloned plasmids. Then, 200 μ L of the broth mixture was spread on an X-gal/IPTG/amp plate. The plates were incubated at 37°C overnight. The next day, plates were examined for white colonies, which indicated cloning had occurred. White colonies were selected using sterile toothpicks and transferred to tubes containing 2mL of LB/amp broth. Tubes were placed in the shaker and incubated at 37°C overnight. DNA was

extracted from the broth using a miniprep procedure (Promega, 2006) for plasmid DNA isolation.

RESULTS

A genetic variant of Charcot-Marie-Tooth (CMT) disease is associated with a profound and progressive form of hereditary deafness. The Trembler-J mouse is an animal model for this type of CMT. Differential display (Figure 14) was used in this study to compare gene expression in 21 day old wild type and Trembler-J mice. The three main components of Differential Display are reverse transcription of an mRNA population using one of three anchor primers, PCR amplification using an arbitrary primer, and denaturing polyacrylamide gel electrophoresis.

RNA Isolation

RNA was successfully isolated from the lung tissue of two Trembler-J mice and two wild type mice. This critical step was the most time consuming due to the unstable nature of RNA. Correct homogenization technique proved to be the key to a successful RNA isolation. Initially, continuous homogenization was performed for several seconds on each sample. This, however, resulted in RNA degradation due to excessive heat generated by the rotor. Homogenization using short pulses proved to be a more successful technique. Quality RNA and degraded RNA are shown in Figure 17.

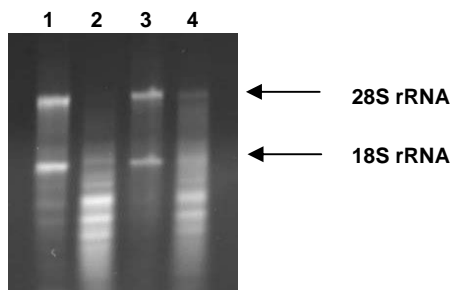


Figure 17: Evaluation of RNA Integrity by Agarose Gel Electrophoresis. Physical integrity of RNA is measured by degradation of the 18S and 28S rRNA. Homogenization using short pulses resulted in quality RNA isolation as is seen in lanes 1 (Trembler-J) and 3 (wild type) by the presence of intact 18S and 28S rRNA. Continuous homogenization for several seconds resulted in degraded rRNA as seen in lanes 2 and 4.

UV Spectrophotometer Quantification

UV Spectrophotometer quantification was used to identify the concentration of RNA in each sample. The ratio of absorbance values at 260 and 280nm ensured RNA purity. Table 3 shows the RNA concentration and A₂₆₀/A₂₈₀ ratio of each sample.

Table 3: RNA Concentration and A₂₆₀/A₂₈₀ of RNA Samples

Mouse ID	Concentration	A₂₆₀/A₂₈₀ Ratio
L2-6 (wild type)	221.48 ug/mL	1.831
L3-9 (wild type)	124.76 ug/mL	1.877
L1-3 (Trembler-J)	501.76 ug/mL	1.754
L3-10 (Trembler-J)	140.31 ug/mL	1.849

Differential Display

Three anchor primers (H-TG, H-TC, H-TA) were used in the reverse transcription reaction to subdivide the transcript population. Each anchor primer binds to the 3' end of the transcript at the poly-A tail. Of the three anchor primers, only two (H-TG, H-TC) yielded differentially displayed bands. A total of 74 differentially expressed transcripts were identified between 21 day control (wild type) and mutant (Trembler-J) samples. PCR reactions using anchor primer H-TG yielded 24 differentially displayed bands (Figure 17). PCR reactions using anchor primer H-TC yielded 50 differentially displayed bands. PCR reactions using anchor primer H-TA did not yield any differentially displayed bands.

PCR reactions using nonspecific arbitrary primers of 13 nucleotides were performed on each of the three cDNA transcript populations. Fourteen arbitrary primers were used in this study. Of the fourteen, arbitrary primers 1, 2, 3, 4, 5, 6, 9, 12 yielded differentially displayed bands. Arbitrary primers 7,8,10,11,13,14, however, did not yield any visually distinct differentially displayed bands.

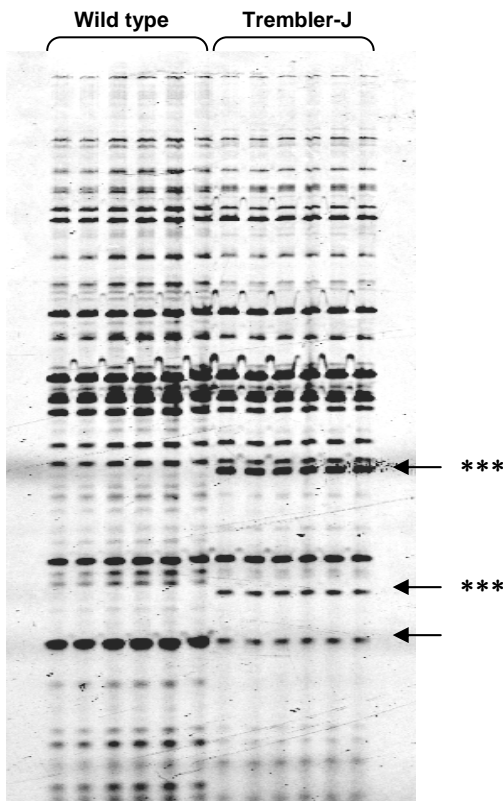


Figure 18: Denaturing Acrylamide Gel Featuring RH-TG Anchor Primer and Arbitrary Primer 4 PCR Products. The above acrylamide gel shows PCR products of wild type and Trembler-J samples using H-TG anchor primer and arbitrary primer 4. The wild type samples are found in the six lanes on the left, and the Trembler-J samples are found in the six lanes on the right. Several differentially displayed transcripts are identified by arrows. The asterisks identify bands that represent up-regulated transcripts in the Trembler-J sample.

There were 42 possible anchor primer and arbitrary primer combinations in this study (3 anchor primers x 14 arbitrary primers = 42 combinations). Of the 42 combinations, only 10 resulted in differentially displayed bands (Table 4).

Combinations of H-TG anchor primer and arbitrary primers 1,2, and 4 resulted in 24 differentially displayed bands, and combinations of H-TC anchor primer and arbitrary primers 2,3,4,5,6,9,and 12 resulted in 50 differentially displayed bands. The most number of bands (16) were found from the combination of H-TG anchor primer and arbitrary primer 4 (Figure 18).

Table 4: Number of DD Bands Resulting from Anchor/Arbitrary Primer Combinations

Anchor Primer	Arbitrary Primer	Number of DD Bands
G	1	6
G	2	2
G	4	16
C	2	6
C	3	6
C	4	8
C	5	10
C	6	12
C	9	4
C	12	4
		Total: 74

DD = Differential Display

Differential Display allows the comparison of gene expression levels in control and mutant samples. Up and down regulation is shown by comparison of the mutant sample to the control sample. In this study, most bands (63 out of 74) were down-regulated in the Trembler-J sample (Table 5). However, 11 bands were up-regulated in the Trembler-J sample (Table 6).

Table 5: Primer Combinations Producing Down-Regulation in Trembler-J PCR Products

Anchor Primer	Arbitrary Primer	Number of Down Regulated Samples
G	1	6
G	2	2
G	4	14
C	2	5
C	3	6
C	4	5
C	5	8
C	6	10
C	9	3
C	12	4

Table 6: Primer Combinations Producing Up-Regulation in Trembler-J PCR Products

Anchor Primer	Arbitrary Primer	Number of Up Regulated Samples
G	4	2
C	2	1
C	4	3
C	5	2
C	6	2
C	9	1

Anchor primer H-TA produced no differentially displayed bands. Figure 19 shows an acrylamide gel with wild type and Trembler-J PCR products from anchor primer H-TA and arbitrary primers 9-14.

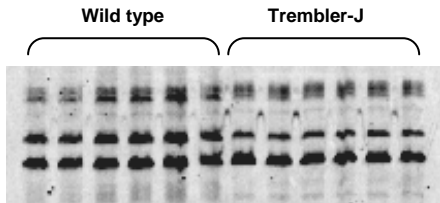


Figure 19: H-TA PCR Products Showing No Differentially Displayed Transcripts. This acrylamide gel displays PCR products of anchor primer H-TA and arbitrary primers 11. Wild type samples are loaded in lanes 1 through 6. Trembler-J samples are loaded in lanes 7 through 12.

PCR-Agarose Purification

Each band of interest was subjected to PCR amplification and agarose purification in preparation for cloning and DNA sequence analysis. Successful amplification and purification of DD products were achieved for 60 of the 74 differentially displayed bands. Fourteen differentially regulated samples were, however, not recoverable upon reamplification. Figure 20 shows a 1.5% agarose gel with the PCR products of several differentially regulated bands.

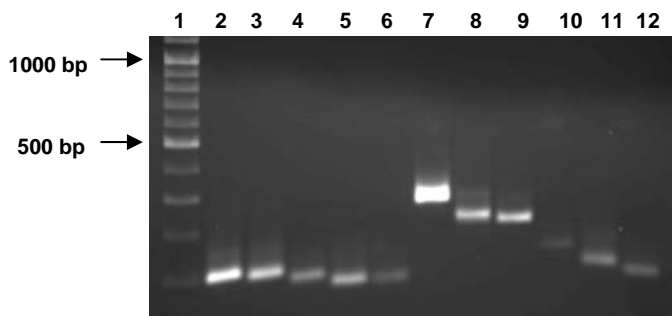


Figure 20: Agarose Gel Showing PCR Products of Differentially Displayed Transcripts. The above 1.5% agarose gel shows PCR products from differentially displayed bands that were the PCR products of anchor primer R-TC and arbitrary primers 2 (lanes 2-6) and 3 (lanes 7-12). Lane 1 shows a 100 bp DNA ladder.

The next phase of the study involves cloning each sample for purification purposes. Isolated clones will be ligated into pUC19 and sequenced in order to identify genes that have shown differential display in the lung tissue of wild type and Trembler-J mice. If time permits, identified genes will be grouped according to structure and function.

DISCUSSION

This study focused on a genetic variant of CMT1A that is uniquely associated with a profound and progressive form of hereditary deafness. The co-presentation of hearing loss with classic peripheral neuropathy in CMT patients is rare and most often associated with point mutations in the PMP22 gene. The exact function of PMP22 is unknown but studies have implicated PMP22 in the formation and myelination of the peripheral nervous system. These observations are consistent with the symptoms and pathology of CMT as well as the high expression levels of PMP22 in neural tissues. PMP22, however, is also widely expressed in non-neural tissues, particularly those of epithelial origin. In these tissues, PMP22 has a characteristic gene expression pattern at periods of growth arrest and terminal differentiation.

Interestingly, the hearing loss described in patients with CMT caused by point mutations shows both a neural and non-neural component. We propose that PMP22 plays a dual role in the development of normal hearing: peripheral myelination of the auditory nerve and regulation of cell growth and differentiation of non-neural cells of the auditory system.

Towards understanding the non-neural role of PMP22, we have compared control (wild type) and mutant (Trembler-J) lung tissue in order to examine the influence of PMP22 on gene expression in non-neural tissues at the 21 day developmental time point.

The majority of differentially displayed transcripts (63 out of 74) were down regulated in the Trembler-J sample (Table 5). However, 11 samples were up regulated in the Trembler-J sample (Table 6). It is not known why a mutation in PMP22 would lead primarily to the down regulation of such genes, but it could be hypothesized that during normal cellular development, PMP22 acts as a transcriptional activator, turning on genes important for cell growth. Consequently, when the protein is mutated one would predict a reduced expression of these genes. DNA sequence identification of these transcripts will aid in developing a model of how PMP22 expression influences cellular development through transcriptional regulation of other genes.

In addition to up and down regulation, DD analysis revealed that certain anchor primer/arbitrary primer combinations produced more differentially displayed transcripts than others (Table 4). The combination of anchor primer R-TG with arbitrary primers 1, 2, and 4 produced 24 differentially displayed bands, while the combination of anchor primer R-TC with arbitrary primers 2, 3, 4, 5, 6, 9, and 12 produced 50 differentially displayed bands. The reason for this is unclear, but further studies may reveal that a G or C in specific positions on the transcript contributes to transcript stability or processing.

We have begun the identification of differentially regulated transcripts by cloning the DD products into pUC19 plasmid. Cloning is necessary to

ensure that multiple transcripts represented by the same DD band are not being sequenced together. Some difficulty has been encountered with cloning the DD products in that insert size of a DD product is typically small (< 300bp) and the cloning is dependent on blunt-end ligation. To drive the ligation reaction, the ratio of DD product: pUC19 vector will be increased and 10mM ATP will be added to the reaction to facilitate the joining of blunt fragments. Once the DD products are cloned, DNA sequence analysis can be preformed. DNA sequence information will be used to conduct a BLAST (Basic Local Alignment Search Tool) (www.ncbi.nlm.nih.gov/BLAST) search which will identify genes containing a sequence homologous to our DNA sequence information. Based on the results of the BLAST search, identified genes will be grouped according to structural and functional characteristics. This information will aid in the creation of a model to explain gene interaction and the effects of PMP22 and its interaction with other genes during development. This information will lead to a greater understanding of the general function of PMP22 in non-neural tissues. This, in turn, will further the understanding of the function of PMP22 in the non-neural development of normal hearing.

REFERENCES

- (2007). Basic Local Alignment Search Tool. www.ncbi.nlm.nih.gov Retrieved March 16, 2007: <http://www.ncbi.nlm.nih.gov/BLAST>
- (2007). Central Dogma of Genetics. www.stanford.edu Retrieved March 16, 2007: <http://cmgm.stanford.edu/biochem201>.
- (2007). Degraded and Intact RNA. www.ambion.com Retrieved March 16, 2007: <http://www.ambion.com>
- Adlkofer K, Martini R, Aguzzi A, Zielasek J, Toyka KV, Suter U. (1995). "Hypermyelination and demyelinating peripheral neuropathy in Pmp22-deficient mice." Nature Genet 11:274-280.
- Attardi LD, Reczek EE, Cosmas C, Damicco EG, McCurrach ME, Lowe SW, Jacks T. (2000). "PERP, An apoptosis-associated target of p53, is a novel member of the PMP-22/Gas3 family." Genes Dev 14:704-718.
- Baechner D, Liehr T, Harneister H, Altenberger H, Grehl H, Suter U, Rautenstrauss B. (1995). "Widespread expression of the peripheral myelin protein (PMP22) in the neural and non-neural tissues during murine development." J Neurosci Res 42:733-741.
- Ben-Porath I, Yanuka O, Benvenisty N. (1998). "Chromosomal mapping of Tmp (Emp I), Xmp (Emp2), and Ymp (Emp3), genes encoding membrane proteins related to Pmp22." Genomics 49:733-741.

- Brancolini C, Marzinotto S, Edomi P, Agostoni E, Fiorentini C, Muller HW, Schneider C. (1999). "Rho-dependent regulation of cell spreading by the tetraspan membrane protein Gas3/PMP22." Mol Biol Cell 10:2441-2459.
- Charcot JM, Marie P. (1886). "Sur une forme particuliere d'atrophie musculaire progressive, souvent familiale, debutante par les peids et les jambs et atteignant plus tard les mains." Rev Med, 6:97-138.
- Coccia EM, Cicala C, Charlesworth A, Ciccarelli C, Rossi GB, Philipson L, Sorrentino V. (1992). "Regulation and expression of a growth arrest-specific gene (gas5) during growth, differentiation and development." Mol Cell Biol 12:3514-3521.
- Cohen MM, Gorlin RJ. (1995). "Epidemiology, etiology, and genetic patterns." In: Gorlin RJ, Toriello HV, Cohen MM, eds. Hereditary Hearing Loss and Its Syndromes. New York: Oxford University Press.
- De Weerdts CJ, Heerspink W. (1974). "Family with Charcot-Marie-Tooth disease showing unusual biochemical, clinical, and genetic features." Eur Neurol 12:256-260.
- Dyck PJ, Chance P, Lebo R, Carney AJ. (1993). "Hereditary motor and sensory neuropathies." In: Dyck PJ, Thomas PK, Griffin JW, Low PA, Polduslo JF (eds) Peripheral neuropathy, 3rd ed. Philadelphia: WB Saunders. P 1094-1136.

- Dyck PJ and Lambert EH. (1968a). "Lower muscle and primary sensory neuron diseases with peroneal muscular atrophy: I. Neurologic, genetic and electrophysiologic findings in hereditary polyneuropathies." Arch. Neurol, 18: 603.
- Dyck PJ and Lambert EH. (1968b). "Lower motor and primary sensory neuron diseases with peroneal muscular atrophy: II. Neurologic, genetic and electrophysiologic findings in various neuronal degenerations." Arch. Neurol., 18: 619.
- Dyck PJ and Ohta M. (1975). "Neuronal atrophy and degeneration predominantly affecting peripheral sensory neurons." In: Dyck, P.J., Thomas, P.K., Lambert E.H. : Peripheral Neuropathy, Toronto: W.B. Saunders.
- Fabbretti E, Edomi P, Brancolini C, Schneider C. (1995). "Apoptotic phenotype induced by overexpression of wild-type gas3/PMP22: its relation to the demyelinating peripheral neuropathy CMT1A." Genes Dev 9:1846-1856.
- Garcia CA, Malamut RE, England JD, Parry GS, Liu P, Lupski JR. (1995). "Clinical variability in two pairs of identical twins with the Charcot-Marie-Tooth disease type 1A duplication." Neurology, 45:2090-2093.
- GenHunter, Inc. (2005). MessageClean Handbook.
- GenHunter, Inc. (2006). RNASpectra Handbook.

- Griffin JW. (1995). Pathologic changes in Charcot-Marie-Tooth disorders. In: Parry GJ, ed. Charcot-Marie-Tooth disorders: A handbook for primary care physicians. Upland, PA: Charcot-Marie-Tooth Association.
- Hamiel OP, Raas-Rothschipd A, Upadhyaya M, Frydman M, Sarova-Pinhas I, Brand N, Passwell JH. (1993.) “Hereditary motor-sensory neuropathy (Charcot-Marie-Tooth disease) with nerve deafness: a new variant.” J Pediatr 123:431-434.
- Harding AE and Thomas PK (1980). “The clinical features of hereditary motor and sensory neuropathy types I and II.” Brain 103:259.
- Ionasescu VV, Searby CC, Ionasescu R, Chatkupt S, Patel N, Koenigsberger R. (1997). “Dejerine-Sottas neuropathy in mother and son with same point mutation of the PMP22 gene.” Muscle Nerve 20:97-99.
- Kaku DA, Parry GJ, Malamut R, Lupski JR, Garcia CA. (1993). “Uniform slowing of conduction velocities in Charcot-Marie-Tooth polyneuropathy.” Muscle Nerve 19: 74-78.
- Kouseff B, Hards AT, Treiber D, Wollner T, Morris C. (1982). “Charcot-Marie-Tooth disease and sensorineural hearing loss: an autosomal dominant trait.” Birth Defects Orig Artic Ser 18:223-228.

- Kovach MJ, Lin JP, Boyadjiev S, Campbell K, Mazzeo L, Herman K, Rimer L, Frank W, Llewellyn B, Jabs E, Gelber D, Kimonis V. (1999). "A Unique Point Mutation in the PMP22 Gene Is Associated with Charcot-Marie-Tooth Disease and Deafness." American Journal of Human Genetics 64:1580-1593.
- Liang P and Pardee A. (1992). "Differential display of eukaryotic messenger RNA by means of the polymerase chain reaction." Science 257:967-971.
- Lupski JR and Garcia CA. (1992). "Molecular genetics and neuropathology of Charcot-Marie-Tooth disease type 1A." Brain Pathol 2:337-490.
- Lupski JR, Garcia CA, Parry GJ, Patel PI. (1991). "Charcot-Marie-Tooth polyneuropathy syndrome: clinical, electrophysiological, and genetic aspects." In: Appel S, editor. Current Neurology. Chicago: Mosby Yearbook.
- Marvin KW, Fujimoto W, Jetten AM. (1995). "Identification and characterization of a novel squamous cell-associated gene related to PMP22." J Biol Chem 270:28910-28916.
- Manfioletti G, Ruaro ME, Del Sal G, Philipson L, Schneider C. (1990). "A growth arrest-specific (gas) gene codes for a membrane protein." Mol Cell Biol 10:2924-2930.
- McKusick VA. (1992). Mendelian Inheritance in Man: catalogs of autosomal dominant, autosomal recessive, and X-linked phenotypes. 10th ed. John Hopkins University Press, Baltimore.

- Morton NE. (1991). "Genetic epidemiology of hearing impairment." Ann NY Acad Sci 630:16-31.
- Murakami T, Garcia C, Reiter L, Lupski J. (1996). "Reviews in Molecular Medicine." Medicine 5:233-250.
- Naef R and Suter U. (1998). "Many facets of the peripheral myelin protein PMP22 in myelination and disease." Microse Res Tech 41:359-371.
- National Diagnostics. (2005). SequaGel Handbook.
- Nicholson G and Nash J. (1993). "Intermediate nerve conduction velocities define X-linked Charcot-Marie-Tooth neuropathy families." Neurology 43: 2558-2564.
- Pentao L, Wise CA, Chinault AC, Patel PI, Lupski JR. (1992). "Charcot-Marie-Tooth type 1A duplication appears to arise from recombination at repeat sequences flanking the 1.5Mb monomer unit." Nature Genet 2:292-300.
- Promega, Inc. (2006). MiniPrep DNA Purification Handbook.
- QIAGEN, Inc. (2006). QIAquick Spin Handbook.
- QIAGEN, Inc. (2001). RNeasy Mini Handbook.
- Raeymaekers P, Timmerman V, Nelis E, De Jonghe P, Hoogendijk JE, Bass F, Barker DF, Martin JJ, De Visser M, Bolhuis PA, Van Broeckhoven C, and the HMSN Collaborative Research Group. (1991). "Duplication in chromosome 17p11.2 in Charcot-Marie-Tooth neuropathy type 1a (CMT1a)." Neuromusc Dis 1:93-97.

- Resendes BL, Williamson RE, Morton CC (2001). "At the speed of sound: Gene discovery in an auditory system." Am J Hum Genet 69:923-935.
- Robertson ND and Morton CC. (1999). "Beginning of a molecular era in hearing and deafness." Clin Genet 55:149-159.
- Roa BB and Lupski JR. (1993). "Molecular basis of Charcot-Marie-Tooth disease type 1A: gene dosage as a novel mechanism for a common autosomal dominant condition (Review)." Am J Med Sci 306:177-184.
- Ron D and Habener JF. (1992). "CHOP, a novel developmentally regulated nuclear protein that dimerizes with transcription factors C/EBP and LAP and functions as a dominant-negative inhibitor of gene transcription." Genes Dev 6:439-453.
- Sabir M and Lyttle D. (1983). "Pathogenesis of pes cavus in Charcot-Marie-Tooth disease." Clin Orthop 175:173-8.
- Sherwood, L. (2004). Human Physiology. (5th ed.). Belmont: Brooks/Cole-Thompson Learning.
- Skre, H. (1974). "Genetic and clinical aspects of Charcot-Marie-Tooth's disease." Clin Genet, 6:98-118.
- Snipes GJ, Suter U, Welcher AA, Shooter EM. (1992). "Characterization of a novel peripheral nervous system myelin protein (PMP-22. SR13)." J Cell Biol 117:225-238.
- Suter U and Nave KA. (1999). "Transgenic mouse models of CMT1A and HNPP." Ann NY Acad Sci 883:247-253.

- Suter U and Snipes GJ. (1995). "Biology and genetics of hereditary motor and sensory neuropathies." Ann Rev Neurosci 18:45-75.
- Suter U, Moskow JJ, Welcher AA, Snipes GJ, Kosaras B, Sidman RL, Buchberg AM (1992) A leucine-to-proline mutation in the putative first transmembrane domain of the 22kDa peripheral myelin protein in the trembler-J mouse. Proc Nat Acad Sci USA 89:4382-4386.
- Taylor V, Welcher AA, Program AE, Suter U. (1995). "Epithelial membrane protein-1, peripheral myelin protein 22, and lens membrane protein 20 define a novel gene family." J Biol Chem 270:28824-28833.
- Timmerman V, Lupski JR, De Jonghe P. (2006). "Molecular Genetics, Biology, and Therapy for Inherited Peripheral Neuropathies." NeuroMolecular Medicine 8:1-2.
- Tobler AR, Notterpek L, Naef R, Taylor V, Suter U, Shooter EM. (1999). "Transport of Trembler-J mutant peripheral myelin protein 22 is blocked in the intermediate compartment and affects the transport of the wild-type protein by direct interaction." J Neurosci 19:2027-2036.
- Tooth HH. (1886). "The peroneal type of progressive muscular atrophy." HK Lewis, London.
- Uncini A, Di Guglielmo G, Di Muzio A, Gambi D, Sabatelli M, Mignogna T, Tonali P, Marzella R, Finelli P, Archidiacono N, Rocchi M. (1995). "Differential electrophysiological features of neuropathies associated with 17p.11.2 deletion and duplication." Muscle Nerve 18: 628-35.

- Valentijn LJ, Baas F, Wolterman RA, Hoogendijk JE, van den Bosch NH, Zorn I, Gabreels Festen AW, de Visser M, Bolhuis PA. (1992). "Identical pointmutations of PMP-22 in Trembler-J mouse and Charcot-Marie-Tooth disease type 1A." Nat Genet 2:288-291.
- Welcher AA, Suter U, De Leon M, Snipes GJ, Shooter EM. (1991). "A myelin protein is encoded by the homologue of a growth arrest-specific gene." Proc Natl Acad Sci USA 88:7195-7199.
- Wulf P and Suter U. (1999). "Embryonic expression of epithelia membrane protein 1 in early neurons." Brain 116:169-180.
- Zhou R, Assouline J, Abbsa P, Messing A, Gantz B. (1995). "Anatomical and physiological measures of auditory system in mice with peripheral myelin deficiency." Hearing Research 88:87-97.
- Zoidl G, Blass-Kampmann S, D'Urso D, Schmalenbach C, Muller HW. (1995). "Retroviral-mediated gene transfer of the peripheral myelin protein PMP22 in Schwann cells: modulation of cell growth." EMBO J 14:1122-1128.

